Published in final edited form as:
Mol Pharm. 2009 ; 6(1): 221–230. doi:10.1021/mp800149s.

Transferrin Receptor-Targeted Lipid Nanoparticles for Delivery of an Antisense Oligodeoxyribonucleotide against Bcl-2

Xiaojuan Yang[†,‡], **Chee Guan Koh**[‡,§], **Shujun Liu**[‖], **Xiaogang Pan**[†,‡], **Ramasamy Santhanam**[‖], **Bo Yu**[‡,§], **Yong Peng**[⊥], **Jiuxia Pang**[‖], **Sharon Golan**[@], **Yeshayahu Talmon**[@], **Yan Jin**[‡], **Natarajan Muthusamy**[ω], **John C. Byrd**[‖,ω], **Kenneth K. Chan**[†,‡,‖], **L. James Lee**[‡,§], **Guido Marcucci**[*,‖,ω], and **Robert J. Lee**[*,†,‡,‖]

[†]Division of Pharmaceutics, College of Pharmacy, The Ohio State University, Columbus, OH 43210, USA

[‡]NSF Nanoscale Science and Engineering Center (NSEC) for Affordable Nanoengineering of Polymeric Biomedical Devices (CANPBD), The Ohio State University, Columbus, OH 43210, USA

[§]Department of Chemical and Biomolecular Engineering, The Ohio State University, Columbus, OH 43210, USA

[‖]NCI Comprehensive Cancer Center (CCC), The Ohio State University, Columbus, OH 43210, USA

[⊥]Department of Molecular and Cellular Biochemistry, The Ohio State University, Columbus, OH 43210, USA

[ω]Division of Hematology and Oncology, The Ohio State University, Columbus, OH 43210, USA

[@]Department of Chemical Engineering, Technion – Israel Institute of Technology, Haifa 32000, Israel

Abstract

Antisense oligonucleotide G3139-mediated down-regulation of Bcl-2 is a potential strategy for overcoming chemoresistance in leukemia. However, the limited efficacy shown in recent clinical trials calls attention to the need for further development of novel and more efficient delivery systems. In order to address this issue, transferrin receptor (TfR)-targeted, protamine-containing lipid nanoparticles (Tf-LNs) were synthesized as delivery vehicles for G3139. The LNs were produced by an ethanol dilution method and lipid-conjugated Tf ligand was then incorporated by a post-insertion method. The resulting Tf-LNs had a mean particle diameter of ~ 90 nm and G3139 loading efficiency of 90.4%. Antisense delivery efficiency of Tf-LNs was evaluated in K562, MV4-11 and Raji leukemia cell lines. The results showed that Tf-LNs were more effective than non-targeted LNs and free G3139 ($p < 0.05$) in decreasing Bcl-2 expression (by up to 62% at the mRNA level in K562 cells) and in inducing caspase-dependent apoptosis. In addition, Bcl-2 down-regulation and apoptosis induced by Tf-LN G3139 were shown to be blocked by excess free Tf and thus were TfR-dependent. Cell lines with higher TfR expression also showed greater Bcl-2 down-regulation. Furthermore, upregulation of TfR expression in leukemia cells by iron chelator deferoxamine resulted in a further increase in antisense effect (up to 79% Bcl-2 reduction in K562 at the mRNA level) and in caspase-dependent apoptosis (by ~ 3-fold) by Tf-LN. Tf-LN mediated

[*]To whom correspondence should be addressed. Robert J. Lee, Division of Pharmaceutics, College of Pharmacy, The Ohio State University, 500 W 12th Ave, Columbus, OH 43210; Tel: 614-292-4172; Fax: 614-292-7766; lee.1339@osu.edu; or Guido Marcucci, Division of Hematology and Oncology, Department of Medicine, The Ohio State University, 320 W 10th Avenue, Columbus, OH 43210. Tel: 614-293-5738; Fax: 614-293-7525; guido.marcucci@osumc.edu.

delivery combined with TfR up-regulation by deferoxamine appears to be a potentially promising strategy for enhancing the delivery efficiency and therapeutic efficacy of antisense oligonucleotides.

Keywords

Transferrin receptor; lipid nanoparticles; protamine; antisense; oligonucleotide; G3139

1. Introduction

Antisense oligonucleotides, typically of 15–20 nucleotides in length, are designed to target specific mRNA sequences through Watson-Crick hybridization, resulting in the destruction or disablement of the target mRNA.[1] G3139 (oblimersen sodium, Genasense™) is an 18-mer phosphorothioate oligonucleotide targeting the anti-apoptotic protein Bcl-2. Since Bcl-2 is frequently overexpressed in tumor cells and is implicated in drug resistance, down-regulation of Bcl-2 using G3139 can potentially restore chemosensitivity in leukemia cells. Combinations of G3139 with chemotherapeutics have recently been studied for the treatment of acute myelogenous leukemia (AML)[2] and chronic lymphocytic leukemia (CLL).[3] However, clinical efficacy of G3139 has been shown to be limited. This might be due to the rapid clearance of G3139 from blood circulation by metabolism and excretion, as well as the low permeability of the drug across the cellular membrane. Although the phosphorothioate backbone of G3139 renders it less sensitive to nucleases, other remaining obstacles in the G3139 delivery pathway still need to be overcome. A possible strategy for improving efficacy of G3139 is through the development and adoption of targeted drug delivery systems.

Nanoscale drug carriers, in the range of 50 – 300 nm in diameter, have shown much promise serve as drug carriers. They are known to accumulate in solid tumors based on the enhanced permeability and retention (EPR) effect.[4,5] In addition, they are not subjected to clearance by renal excretion and typically exhibit prolonged systemic circulation time. A series of lipid-based nanocarriers have been developed for systemic nucleic acid delivery, such as stabilized plasmid-lipid particles (SPLPs),[6–8] pre-condensed stabilized plasmid lipid particles (pSPLPs)[9] and stabilized nucleic-acid-lipid particles (SNALPs).[10]

Another strategy for oligonucleotide delivery is via electrostatic complexation with a polycation. Protamine sulfate, a polycationic peptide (MW 4.5 kDa), can bind oligonucleotides to form 100–200 nm particles, also known as “proticles”, via electrostatic interactions. These have been shown to efficiently deliver the oligonucleotide into the nucleus[11] and to protect oligonucleotides against serum nucleases.[12–14] Proticles, however, have poor colloidal stability.[12]

To achieve selective targeting of tumor cells, ligands like antibodies,[15,16] transferrin (Tf)[17,18] and folate[19] have been conjugated to nanocarriers. Tf receptor (TfR) is a dimeric transmembrane glycoprotein (180 kDa) frequently up-regulated in proliferating cells, including a majority of tumor cells.[20,21] TfR is further up-regulated upon iron depletion by chelator deferoxamine. The ligand for TfR, Tf, is an 80 kDa iron-transporting glycoprotein that can be taken up by cells via TfR-mediated endocytosis.[17,22,23] Tfconjugated cationic polymers or cationic liposomes have been studied previously for delivery of both plasmid DNA and oligonucleotides.[17,18,24] In this study, we developed a novel oligonucleotide carrier, Tf-LNs, which incorporated Tf as targeting ligand and protamine as an oligonucleotide complexing agent. These LNs showed excellent physiochemical properties and oligonucleotide delivery efficiency. The Tf-LNs, loaded with G3139, were evaluated for

Bcl-2 downregulation and pro-apoptotic activities in leukemia cell lines. Tf-LNs were shown to have high efficiency and TfR specificity in delivery of G3139 and effectively reduced Bcl-2 expression and increased cell apoptosis among leukemia cells. Furthermore, the delivery efficiency via Tf-LNs was further enhanced by deferoxamine, which up-regulated TfR expression on leukemia cells.

2. Materials and Methods

2.1. Reagents

3β-[N-(N',N'-dimethylaminoethane)-carbamoyl] cholesterol (DC-chol), egg phosphatidylcholine (egg PC) and distearoyl phosphatidylethanolamine-N-[maleimide-polyethylene glycol, MW 2000] (Mal-PEG_{2000}-DSPE) were purchased from Avanti Polar Lipids (Alabaster, AL). Methoxy-PEG_{2000}-DSPE (PEG_{2000}-DSPE) was purchased from Genzyme Corporation (Cambridge, MA). Human holo-transferrin (Tf), 2-iminothiolane (Traut's reagent), protamine sulfate, and other chemicals were purchased from Sigma Chemical Co. (St. Louis, MO). All tissue culture media and supplies were purchased from Invitrogen (Carlsbad, CA).

2.2 Antisense oligonucleotides

All oligonucleotides used in this study were fully phosphorothioated. G3139 (5'-TCT CCC AGC GTG CGC CAT-3') and its fluorescence-labeled derivative, G4243 (FITC-G3139), were generously provided by Genta Inc. (Berkeley Heights, NJ) or were custom synthesized by alpha-DNA (Montreal, QC, Canada).

2.3. Cell culture

All leukemia cell lines were cultured in RPMI 1640 media supplemented with 10% heat-inactivated fetal bovine serum (FBS) (Invitrogen), 100 U/mL penicillin, 100 μg/mL streptomycin, and L-glutamine at 37 °C in a humidified atmosphere containing 5% CO_2.

2.4. Preparation of Tf-conjugated G3139-containing LNs (Tf-LNs)

An ethanol dilution method[8] was modified for the synthesis of LNs containing G3139, as illustrated in Figure 1. Briefly, a lipid mixture egg PC/DC-Chol/PEG_{2000}-DSPE at molar ratios of 65/30/5 was dissolved in ethanol (EtOH), and then mixed with protamine in a citrate buffer (20 mM, pH 4) at ratios for lipid:protamine of 12.5:0.3 (w/w) and EtOH:water of 2:1 (v/v). G3139 was dissolved in citrate buffer (20 mM, pH 4) and then added into the lipid/protamine solution under vortexing to spontaneously form "pre-LNs" at an EtOH concentration of 40% (v/v). The complexes were then dialyzed against citrate buffer (20 mM, pH 4) at room temperature for 2 hours and then against HEPES-buffered saline (HBS, 20 mM HEPES, 145 mM NaCl, pH 7.4) overnight at room temperature, using a MWCO 10,000 Dalton Spectra/Por Float-A-Lyzer (Spectrum Labs, Rancho Dominguez, CA) to remove free G3139 and to adjust the pH to the physiological range. A postinsertion method[18,24,25] was adopted to incorporate lipid-conjugated Tf ligand into G3139- loaded LNs. Briefly, holo-(diferric)Tf in HEPES-buffered saline (HBS, pH 8, containing 5mM EDTA) was reacted with 5× Traut's reagent to yield holo-Tf-SH. Free Traut's reagent was removed by dialysis using a MWCO 10,000 Dalton Float-A-Lyzer and against HBS. Holo-Tf-SH was coupled to micelles of Mal-PEG_{2000}-DSPE at a protein-tolipid molar ratio of 1:10. The resulting Tf-PEG_{2000}-DSPE micelles were then incubated with the G3139-loaded LNs for 1 hour at 37°C at Tf-PEG_{2000}-DSPE-to-total lipid ratio of 1:100. For synthesis of fluorescence-labeled LNs, G3139 was spiked with 10% fluorescent oligonucleotide FITC-G3139. As a reference control, protamine-free liposomal G3139 (Lip-G3139) and Tf-Lip-G3139 were also prepared using essentially the same procedure except for omission of

protamine from the formulation and an increase in DC-Chol content to maintain the overall cationic/anionic charge ratio.

The number of bound Tf per LN (molecules per vesicle) was calculated on the basis of the formula (A/B)*C, where A, B and C represent the total number of Tf molecules in a LN suspension, the total number of lipid molecules in a LN suspension, and the number of lipid molecules per LN, respectively.[26] The particle size of Tf-LNs was analyzed on a NICOMP Particle Sizer Model 370 (Particle Sizing Systems, Santa Barbara, CA). The zeta potential (ξ) of the LNs was determined on a ZetaPALS (Brookhaven Instruments Corp., Worcestershire, NY). All measurements were carried out in triplicates.

2.5. G3139 entrapment efficiency

G3139 concentration was determined by dissolution of the LNs using 0.5% SDS followed by fluorometry to determine fluorescence derived from FITC-G3139, using excitation at 488 nm and emission at 520 nm. G3139 concentration was calculated based on a standard curve of fluorescence intensity versus oligonucleotide concentration. Loading efficiency of G3139 in the LNs was calculated based on the ratio of G3139 concentration in the LN preparation before and after dialysis.

2.6. Cryogenic transmission electron microscopy (cryo-TEM)

Vitrified specimens for cryo-TEM imaging were prepared in a controlled environment vitrification system (CEVS) at 25 °C and 100% relative humidity. Briefly, a drop of the liquid to be studied was applied onto a perforated carbon film, supported by a copper grid and held by the CEVS tweezers. The sample was blotted and immediately plunged into liquid ethane at its melting point (−183 °C). The vitrified sample was then stored under liquid nitrogen (−196 °C) and examined in a Philips CM120 YEM microscope (Eindhoven, The Netherlands), operated at 120 kV, using an Oxford CT-3500 cooling-holder (Abingdon, England). Specimens were equilibrated in the microscope at about −180 °C, examined in the low-dose imaging mode to minimize electron beam radiation damage, and recorded at a nominal underfocus of 4–7 μm to enhance phase contrast. Images were recorded digitally by a Gatan 791 MultiScan CCD camera, and processed using the Digital Micrograph 3.1 software package. Further image processing was performed using the Adobe PhotoShop 5.0 package.

2.7. Colloidal and serum stability of Tf-LNs

The colloidal stability of Tf-LNs was evaluated by monitoring changes in the mean particle diameter during storage at 4 °C. To evaluate the ability of the Tf-LNs to retain G3139 and protect it against nuclease degradation, the formulation was mixed with FBS at a 1:4 (v/v) ratio and incubated at 37 °C. At various time points, aliquots of each sample were loaded onto a ureapolyacrylamide gel (Invitrogen). Electrophoresis was performed and G3139 bands were visualized by SYBR Gold (Invitrogen) staining. The densities of G3139 band were measured and analyzed by the ImageJ software.

2.8. Cellular uptake of Tf-LN G3139

Cellular uptake of Tf-targeted LNs and non-targeted control LNs, loaded with G3139 spiked with 10% fluorescent oligonucleotide FITC-G3139, was evaluated in MV4-11 cells. For the studies, 4×10^5 cells were incubated with 1 μM G3139 entrapped in Tf-LNs at 37 °C. After 4-hour incubation, the cells were washed three times with PBS, by pelleting of the cells at 1,000× g for 3 minutes, aspiration of the supernatant, followed by re-suspension of the cells in PBS. The cells were examined on a Nikon fluorescence microscope (Nikon, Küsnacht, Switzerland), or stained by 4',6-diamidino-2-phenylindole (DAPI), a nuclear counterstain,

and then examined on a Zeiss 510 META Laser Scanning Confocal microscope (Carl Zeiss Inc., Germany). G3139 uptake in leukemia cells was measured by flow cytometry on a FACSCalibur flow cytometer (Becton Dickinson, Franklin Lakes, NJ).

2.9. Measurement of TfR expression on cell surface

TfR expression levels in leukemia cell lines were analyzed based on cellular binding of FITC-Tf determined by flow cytometry. Briefly, 4×10^5 leukemia cells were washed with RPMI media containing 1% BSA and then incubated with 200 μg/ml FITC-Tf at 4 °C for 30 minutes. The cells were then washed twice with cold PBS (pH 7.4) containing 0.1% BSA, by pelleting of the cells at 1,000× g for 3 minutes, aspiration of the supernatant, followed by resuspension of the cells in PBS. Finally, cellular fluorescence was then measured by flow cytometry.

2.10. Transfection studies

Leukemia cells were plated in 6-well tissue culture plates at 10^6/well in RPMI 1640 medium containing 10% FBS. An appropriate amount of Tf- LNs or control formulations was added into each well to yield a final G3139 concentration of 1 μM. After 4-hour incubation at 37 °C in a CO_2 incubator, the cells were transferred to fresh medium, incubated for another 48 hours, and then analyzed for Bcl-2 mRNA level by real-time RT–PCR, for Bcl-2 protein level by Western blot, and for apoptosis by measuring caspase-9 activity, respectively.

2.11. Quantification of Bcl-2 mRNA level by Real-time RT-PCR

The bcl-2 mRNA level in leukemia cells was evaluated using real time RT–PCR, as previously described.[27] Briefly, total RNA was extracted using Trizol reagent (Invitrogen) and cDNA was synthesized by incubating RNA with random hexamer primer (Perkin Elmer, Boston MA), and then with reverse transcriptase (Invitrogen), reaction buffer, dithiothreitol, dNTPs and RNAsin, followed by incubation at 42 °C for 60 minutes and 94 °C for 5 minutes in a thermal cycler (Applied Biosystems, Foster City, CA). The resulting cDNA was amplified by real-time PCR (ABI Prism 7700 Sequence Detection System, Applied Biosystems) using bcl-2 primers and probes (forward primer CCCTGTGGATGACTGAGTACCTG; reverse primer CCAGCCTCCGTTATCCTGG; probe CCGGCACCTGCACACCTGGA). Housekeeping gene ABL mRNAs were also amplified concurrently and to which Bcl-2 mRNA were normalized.

2.12. Quantification of Bcl-2 protein by Western blot

Western blot was carried out as described previously[28]. Briefly, untreated and G3139-treated cells were harvested at 24 or 48 hours after transfection and whole cellular lysates were prepared by lysing the cell in 1× cell lysis buffer containing a protease inhibitor cocktail (CalBiochem, San Diego, CA). Approximately 20 μg of cellular protein was used for immunoblotting using a monoclonal murine anti-human Bcl-2 (Dako, Carpinteria, CA) antibody. Bcl-2 protein expression levels were quantified by ImageJ software and were normalized to the β-actin levels from the same samples.

2.13. Analysis of apoptosis by caspase activation

To analyze cellular apoptosis, caspase-9 activities were measured on untreated and Tf-LN-G3139-treated cells using the caspase Glo-9 assay kit (Promega).[29] Briefly, 5×10^3 cells were plated in a white-walled 96-well plate, and the Z-DEVD reagent, a luminogenic caspase-9 substrate, was added with a 1:1 ratio of reagent to cell solution. After 90 minutes at room temperature, the substrate was cleaved by activated caspase-9, and the intensity of a luminescent signal was measured by a Fluoroskan Ascent FL luminometer (Thermo

Electron Corp.). Differences in caspase-9 activity in Tf-LN-G3139-treated cells compared with untreated cells were determined by fold-change in luminescence.

2.14. Statistical analysis

Data obtained were represented as mean ± standard deviations (S.D.). Comparisons between groups were made by 2-tailed Student's t-tests using the MiniTAB software (Minitab Inc., State College, PA). $p < 0.05$ was used as the cutoff for defining statistically significant differences.

3. Results

3.1. Physical chemical properties of the Tf-LNs

In order to increase the efficiency and specificity of G3139 delivery, Tf-LNs were synthesized. Figure 1 shows the ethanol dilution method used for Tf-LN synthesis[8] and the post-insertion of the Tf ligand.[18]

Particle size values, zeta potential values, and G3139 entrapment efficiencies of LN formulations are presented in Table 1. The particle size and zeta potential of LNs with protamine were 78.1 nm and 5.7 mV and those of G3139-entrapping liposomes without protamine (Lips) were 112.5 nm and 2.0 mV, respectively. This showed that addition of protamine into the formulation resulted in a reduced particle size. Incorporation of Tf into LNs by post-insertion increased the particle size to 90.2 nm but did not significantly alter the zeta potential. The density of Tf on the resulting Tf-LN was estimated to be ~ 46 Tf molecules per particle. The G3139 entrapment efficiencies of the formulations were also determined. The G3139 entrapment efficiency of LN and Tf-LN were 95.9±0.1% and 90.4±0.7%, respectively. These values were significantly greater than those for Lips and Tf-Lips without protamine, which were 76.1±0.2% and 71.9±1.1%, respectively. These results indicated that the incorporation of protamine in the formulation also increased the G3139 entrapment efficiency, whereas the insertion of Tf had only a minor effect on the G3139 entrapment efficiency.

The morphology of LNs before transferrin incorporation was studied by cryo-TEM. As shown in Figure 2, the LNs exhibited several coexisting nanostructures: empty bilayers liposomes (white arrowheads figure 2A), lamellar onion-like structures, and amorphous aggregates. In Figure 2A, the white arrows showed amorphous aggregates that were attributed to the prior aggregation of protamine and ODN. The onion-like spherical particles containing one to several lamellae were indicated by a black arrow, and enlarged in Figure 2B. The lamellar layers were distinct by different contrast of the lipids bilayer and the condensed ODN layer. Due to the affinity of the G3139s to the cationic lipid component, it was probable that they were bound to lipid bilayers, and were sandwiched between adjacent lipid bilayers. Weisman et al. reported similar structures.[30] In Figure 2C, an aggregate with two thick resolved layers was shown. The layers are much thicker than the lamellas of the onion-like structures. These thicker layers were formed probably due to prior aggregation of the ODNs with protamine, which afterwards attaches to the surface of the lipids bilayers.

3.2. Colloidal and serum stability of Tf-LNs

The colloidal stability of G3139-loaded Tf-LNs was evaluated by monitoring changes in the mean diameter during storage in HBS buffer at 4 °C. It was found that the LNs and Tf-LNs remained stable and no significant particle size changes were observed for 12 weeks at 4 °C (Figure 3 Panel A). Meanwhile, Lips and Tf-Lips exhibited less colloidal stability with 32.6% and 33.6% increase in size in the same time period, respectively. In addition, protamine-G3139 complexes with the same protmaine:ODN weight ratio of 3:1 but without

the lipid components aggregated over time under the storage condition. These results indicated that the combination of lipids and protamine is required for colloidal stability of the nanoparticle formulation.

To evaluate the ability of the Tf-LNs both to retain G3139 and to protect it from degradation by nucleases, the formulations were incubated in FBS at 37 °C. At various time points, samples were collected and analyzed by urea-polyacrylamide gel electrophoresis. As shown in Figure 4, the amount of intact G3139 remaining in Tf-LN decreased slowly with incubation time. After 12 hours of exposure to serum, ~ 80 % of G3139 remained intact in Tf-LNs, whereas < 10% of G3139 remained in the Lip formulation. Interestingly, Tf-Lips, although less stable in serum than Tf-LNs, retained 42% of loaded G3139 over the same incubation time frame.

3.3. Cellular uptake of Tf-LN-G3139

Cellular uptake of Tf-LN-G3139, containing 10% fluorescent FITC-G3139, was evaluated in MV4-11 cells. By confocal microscopy, it was found that, after 15-minute incubation, most of the G3139 was bound to the cellular membrane. At 1 hour, the Tf-LNs were mostly internalized (Figure 5 Panel A). Tf-LN G3139 was efficiently internalized by the cells and the level of uptake was much higher than that of free G3139 (Figure 5 Panel B and C). As a non-targeted control, delivery of G3139 via LNs was also evaluated. LN G3139 exhibited lower uptake compared to the Tf-LNs, suggesting that the enhancement of G3139 cellular uptake via Tf-LN was due to the presence of Tf ligands on the surface of LNs. In addition, Tf-LN mediated delivery was shown to be blocked by excess free holo-Tf (Figure 5 Panel D), indicating that the increase in uptake was TfR specific. To investigate the role of TfR expression level in Tf-LN-G3139 cellular uptake, K562 cells were treated with 20 μM of deferoxamine, an iron chelator known to up-regulate cellular TfR expression, for 18 hours. These cells displayed a 3.3-fold higher level of Tf-LN-G3139 cellular uptake compared those that were untreated (Figure 5 Panel E).

3.4. Tf-LN-G3139 mediated Bcl-2 down-regulation

TfR expression on leukemia cell lines K562, MV4-11 and Raji, with or without deferoxamine treatment are shown in Figure 6A. TfR expression was increased upon deferoxamine treatment in all three cell lines. The leukemia cells were incubated with Tf-LN-G3139 for 48 hours. Real time RT- PCR and Western blot were performed for Bcl-2 mRNA level and protein expression determination, respectively. As shown in Figure 6B, different cell lines had varied responses in Bcl-2 expression at the mRNA level. Bcl-2 mRNA reduction following treatment with Tf-LN-G3139 was 41% in MV4-11 cells compared to 26% following treatment with non-targeted LNs and 6% with free G3139. In K562 cells the Tf-LNs produced as high as 62% down-regulation of Bcl-2 at mRNA level, which was 2.2 times greater than that achieved by non-targeted LN. These demonstrated a more efficient down-regulation of Bcl-2 by the Tf-LNs. The same trend was observed based on the Bcl-2 protein level. As shown in Figure 6C, Tf-LN mediated the greatest reduction of Bcl-2 protein levels in all the cell lines studied compared to free G3139 and non-targeted LNs. For example, in K562 cells, Tf-LNs produced 54% down-regulation of Bcl-2 protein, which was 1.3 times and 50.2 times higher than that by non-targeted LN and free G3139, respectively. In addition, we found that reductions in Bcl-2 expression by Tf-LNs were correlated with the TfR expression levels on cell surface. For example, K562 cells, which had the highest TfR expression levels among the studied leukemia cell lines (Figure 6A), also showed the highest (65%) reduction in Bcl-2 at protein level. Interestingly, 20 μM free holo-Tf effectively blocked Bcl-2 down-regulation by Tf-LN-G3139 in K562 cells (Figure 6D). This result indicated that Tf-LN mediated delivery of G3139 was dependent on TfR expression. Moreover, the increased TfR expression by deferoxamine in different leukemia

cell lines (Figure 6A) resulted in greater inhibition of Bcl-2 expression by Tf-LN-G3139 (Figure 6B&C), further indicating that the delivery was TfR-dependent.

3.5. Tf-LNs containing G3139 exhibited pronounced effect on cell apoptosis

Having demonstrated knockdown of the anti-apoptotic protein Bcl-2, we next sought to determine the effect of Tf-LNs containing G3139 on cellular apoptosis. Leukemia K562 cells were treated with the Tf-LNs. We observed, by confocal microscopy, that G3139 accumulated inside the cells after 1-hour treatment. At 240 minutes, nuclei in some of the cells were fragmented, indicating the occurrence of apoptosis in these cells (Figure 5A). At 48 hours after the treatment, the cells were collected and analyzed for caspase-9 activities. As shown in Figure 7, caspase-9 activity in cells treated with Tf-LN-G3139 was 2× higher than in those treated by non-targeted LN and 43× higher than those treated by free G3139, indicating markedly enhanced apoptosis induction by the Tf-LNs. Pretreatment of K562 cells by deferoxamine further increased caspase-9 activity to 3× that of untreated cells, suggesting that the enhanced apoptosis by Tf-LN-G3139 was TfR level-dependent.

4. Discussion

Bcl-2 is a key apoptosis-regulating protein that has been implicated in mechanisms of chemoresistance by a variety of malignancies by blocking programmed cell death. G3139 is an antisense oligonucleotide that can down-regulate Bcl-2 expression, thus potentially act as a chemosensitization agent. However, effective therapy requires efficient G3139 delivery. The objective of this study was to develop TfR-targeted LNs that exhibit collidal stability and that have high efficiency and selectivity in G3139 delivery to leukemia cells. The LNs incorporated both protamine and lipids. Tf was incorporated to provide TfRmediated leukemia cell targeting. These nanoparticles were shown to efficiently deliver G3139 to TfR-positive leukemia cells, as shown by effective down-regulation of Bcl-2.

It has been noted that there is a relatively high concentration of Tf in circulation, which may block TfR-mediated targeting strategies in vivo. However, most of the circulating Tf is not iron-loaded and, therefore, have a much lower affinity for the TfR compared to the holo-Tf used in the Tf-LNs. In fact, gallium-67 citrate, a clinical radiopharmaceutical designed for selective tumor imaging, has been shown to act by in vivo loading on to circulating Tf and to selectively target tumors in patients.[31] This shows that Tf-based TfR targeting strategies can be effective in vivo despite the presence of an abundance of the unloaded Tf in circulation. In addition, Tf-LNs contain multiple Tfs on each particle and are capable of multivalent interaction with the target cells. Such interaction is likely to result in a great increase in affinity compared to the Tf found in circulation, which is monovalent. Therefore, the Tf-LNs should be able to out-compete endogenous Tf found in circulation for TfR binding.

The lipid composition used in this study was egg PC/DC-Chol/PEG_{2000}-DSPE (molar ratio 65/30/5). The utilizations of both protamine and DC-Chol as positive charged components ensured high G3139 loading efficiencies. During LN assembly, G3139 was mixed with protamine and cationic lipids. It was possible that, due to the faster diffusion rate and charge density of protamine compared to Lips, the ODN would first interact with protamine and then the resulting complexes are stabilized by further coating of the lipids. The Tf-PEG-DSPE introduced by post-insertion is likely distributed on the surface of the nanoparticles. In this process, the micelles were disassembled and their components were incorporated into the bilayers of the LNs. The structure of the LNs, as shown by the cryo- TEM image, was very similar to those of pSPLPs, which has been described previously.[8] When pH was adjusted to 7.5 upon removal of EtOH by dialysis, the head group of DC-Chol became

partially deprotonated. The zeta potential of the resulting LNs following dialysis was low (5.7 mV).

An important property of the LNs is excellent colloidal stability. This is likely due to the high DNA binding activity of protamine and surfactant characteristics of the lipids. PEG_{2000}-DSPE in the formulation provided steric stabilization of the LNs. Tf conjugate may also contribute to LN stability in serum by shielding them from interactions with plasma proteins. Pre-mixing of protamine with lipids was found to be critical for small particle formation since G3139/protamine complexes in the absence of lipids aggregated over time. In addition, pre-mixing of protamine with G3139 and then adding this mixture into the lipids also resulted in unstable particles that aggregated over time. Using the above described formulation, G3139 encapsulation efficiencies were 95.9% and 90.4% for LN and Tf-LN, respectively. Therefore, the LN formulation is much superior to protamine-oligonucletide and lipid-oligonucleotide complexes both in terms of DNA loading efficiency and colloidal stability.

To investigate G3139 delivery efficiency via Tf-LNs, Bcl-2 down-regulation was evaluated in 3 different leukemia cell lines (K562, MV4-11 and Raji), followed by the measurement of caspase-dependent apoptosis in K562 cells. TfR expression level was found to be an important factor in determining the efficiency of G3139 delivery by Tf- LNs. Deferoxamine, a clinically used iron chelator for the treatment of secondary iron overload, is known to up-regulate TfR expression in cells. Therefore, deferoxamine should increase TfR-targeting efficiency of the Tf-LNs. This was confirmed by the enhanced Bcl-2 down regulatory activities of the deferoxamine-treated leukemia cells by Tf-LNs. Positive correlation between Bcl-2 down-regulation by Tf-LN and enhancement of TfR expression by deferoxamine suggests a potentially promising novel strategy for enhancing delivery and therapeutic efficacy of antisense oligonucleotides.

5. Conclusions

A stable, TfR-targeted LN formulation encapsulating antisense G3139 was synthesized and evaluated. The LNs exhibited excellent G3139 loading efficiency and colloidal stability and protected G3139 against degradation by serum nucleases. Tf-LNs showed efficient delivery of G3139 to TfR-positive leukemia cells, which can be blocked by excess free Tf. Deferoxamine treatment increased TfR expression and enhanced the transfection activity of Tf-LNs. Combining defeoxamine pretreatment with Tf-LN mediated delivery is a promising strategy for targeted delivery of G3139 and other antisense drugs to leukemia cells.

Acknowledgments

This work was support in part by NSF grant EEC-0425626 and NIH grant R01 CA135243. We wish to thank Dr. Robert Brown at Genta for providing us with oligonucleotides G3139 and G4243 (FITC-G3139).

References

1. Crooke ST. Progress in antisense technology. Annu. Rev. Med. 2004; 55:61–95. [PubMed: 14746510]
2. Moore J, Seiter K, Kolitz J, Stock W, Giles F, Kalaycio M, Zenk D, Marcucci G. A Phase II study of Bcl-2 antisense (oblimersen sodium) combined with gemtuzumab ozogamicin in older patients with acute myeloid leukemia in first relapse. Leuk Res. 2006; 30:777–783. [PubMed: 16730060]
3. Cheson BD. Oblimersen for the treatment of patients with chronic lymphocytic leukemia. Ther Clin Risk Manag. 2007; 3:855–870. [PubMed: 18473009]
4. Naoto O, Atsushi T, Toshiyuki T, Yukihiro N, Toshiyuki S, Fumiaki I, Shoji O. Preparation of RES-Avoiding liposomes. J. Pharmacobio-Dynamics. 1992; 15 69-69.

5. Seymour LW. Passive tumor targeting of soluble macromolecules and drug conjugates. Crit. Rev. Ther. Drug Carr. Syst. 1992; 9:135–187.
6. Wheeler JJ, Palmer L, Ossanlou M, MacLachlan I, Graham RW, Zhang YP, Hope MJ, Scherrer P, Cullis PR. Stabilized plasmid-lipid particles: construction and characterization. Gene Ther. 1999; 6:271–281. [PubMed: 10435112]
7. Zhang YP, Sekirov L, Saravolac EG, Wheeler JJ, Tardi P, Clow K, Leng E, Sun R, Cullis PR, Scherrer P. Stabilized plasmid-lipid particles for regional gene therapy: formulation and transfection properties. Gene Ther. 1999; 6:1438–1447. [PubMed: 10467368]
8. Jeffs LB, Palmer LR, Ambegia EG, Giesbrecht C, Ewanick S, MacLachlan I. A scalable extrusion-free method for efficient liposomal encapsulation of plasmid DNA. Pharm. Res. 2005; 22:362–372. [PubMed: 15835741]
9. Heyes J, Palmer L, Chan K, Giesbrecht C, Jeffs L, MacLachlan I. Lipid encapsulation enables the effective systemic delivery of polyplex plasmid DNA. Mol. Ther. 2007; 15:713–720. [PubMed: 17299407]
10. Morrissey DV, Lockridge JA, Shaw L, Blanchard K, Jensen K, Breen W, Hartsough K, Machemer L, Radka S, Jadhav V, Vaish N, Zinnen S, Vargeese C, Bowman K, Shaffer CS, Jeffs LB, Judge A, MacLachlan I, Polisky B. Potent and persistent in vivo anti-HBV activity of chemically modified siRNAs. Nat. Biotechnol. 2005; 23:1002–1007. [PubMed: 16041363]
11. Sorgi FL, Bhattacharya S, Huang L. Protamine sulfate enhances lipidmediated gene transfer. Gene Ther. 1997; 4:961–968. [PubMed: 9349433]
12. Junghans M, Kreuter J, Zimmer A. Antisense delivery using protamine-oligonucleotide particles. Nucleic Acids Res. 2000; 28:E45. [PubMed: 10773093]
13. Gao X, Huang L. Potentiation of cationic liposome-mediated gene delivery by polycations. Biochemistry. 1996; 35:1027–1036. [PubMed: 8547238]
14. Li S, Huang L. In vivo gene transfer via intravenous administration of cationic lipid-protamine-DNA (LPD) complexes. Gene Ther. 1997; 4:891–900. [PubMed: 9349425]
15. Leserman LD, Machy P, Barbet J. Cell-specific drug transfer from liposomes bearing monoclonal-antibodies. Nature. 1981; 293:226–228. [PubMed: 7278980]
16. De Menezes DEL, Pilarski LM, Allen TM. In vitro and in vivo targeting of immunoliposomal doxorubicin to human B-cell lymphoma. Cancer Res. 1998; 58:3320–3330. [PubMed: 9699662]
17. Singh M. Transferrin as a targeting ligand for liposomes and anticancer drugs. Curr. Pharm. Design. 1999; 5:443–451.
18. Chiu SJ, Liu SJ, Perrotti D, Marcucci G, Lee RJ. Efficient delivery of a Bcl-2-specific antisense oligodeoxyribonucleotide (G3139) via transferrin receptor-targeted liposomes. J. Control. Release. 2006; 112:199–207. [PubMed: 16564596]
19. Lee RJ, Low PS. Delivery of liposomes into cultured KB cells via folate receptor-mediated endocytosis. J. Biol. Chem. 1994; 269:3198–3204. [PubMed: 8106354]
20. Borhani DW, Harrison SC. Crystallization and X-Ray-diffraction studies of a soluble form of the human transferrin receptor. J. Mol. Biol. 1991; 218:685–689. [PubMed: 2023243]
21. Trowbridge IS, Omary MB. Human cell-surface glycoprotein related to cell-proliferation is the receptor for transferrin. PNAS. 1981; 78:3039–3043. [PubMed: 6265934]
22. MacGillivray RT, Mendez E, Shewale JG, Sinha SK, Lineback-Zins J, Brew K. The primary structure of human-serum transferrin - the structures of 7 cyanogen-bromide fragments and the assembly of the complete structure. J. Biol. Chem. 1983; 258:3543–3553. [PubMed: 6833213]
23. Bailey S, Evans RW, Garratt RC, Gorinsky B, Hasnain S, Horsburgh C, Jhoti H, Lindley PF, Mydin A, Sarra R. Molecular-structure of serum transferrin at 3.3-a resolution. Biochemistry. 1988; 27:5804–5812. [PubMed: 3179277]
24. Xu LA, Pirollo KF, Tang WH, Rait A, Chang EH. Transferrin-liposome-mediated systemic p53 gene therapy in combination with radiation results in regression of human head and neck cancer xenografts. Hum. Gene Ther. 1999; 10:2941–2952. [PubMed: 10609655]
25. Allen TM, Sapra P, Moase E. Use of the post-insertion method for the formation of ligand-coupled liposomes. Cell Mol. Biol. Lett. 2002; 7:889–894. [PubMed: 12378272]

26. Ishida O, Maruyama K, Tanahashi H, Iwatsuru M, Sasaki K, Eriguchi M, Yanagie H. Liposomes bearing polyethyleneglycol-coupled transferrin with intracellular targeting property to the solid tumors in vivo. Pharm. Res. 2001; 18:1042–1048. [PubMed: 11496943]
27. Marcucci G, Livak KJ, Bi W, Strout MP, Bloomfield CD, Caligiuri MA. Detection of minimal residual disease in patients with AML1/ETO-associated acute myeloid leukemia using a novel quantitative reverse transcription polymerase chain reaction assay. Leukemia. 1998; 12:1482–1489. [PubMed: 9737700]
28. Liu S, Liu Z, Xie Z, Pang J, Yu J, Lehmann E, Huynh L, Vukosavljevic T, Takeki M, Klisovic RB, Baiocchi RA, Blum W, Porcu P, Garzon R, Byrd JC, Perrotti D, Caligiuri MA, Chan KK, Wu LC, Marcucci G. Bortezomib induces DNA hypomethylation and silenced gene transcription by interfering with Sp1/NF-kappaB-dependent DNA methyltransferase activity in acute myeloid leukemia. Blood. 2008; 111:2364–2373. [PubMed: 18083845]
29. Neviani P, Santhanam R, Oaks JJ, Eiring AM, Notari M, Blaser BW, Liu S, Trotta R, Muthusamy N, Gambacorti-Passerini C, Druker BJ, Cortes J, Marcucci G, Chen CS, Verrills NM, Roy DC, Caligiuri MA, Bloomfield CD, Byrd JC, Perrotti D. FTY720, a new alternative for treating blast crisis chronic myelogenous leukemia and Philadelphia chromosome-positive acute lymphocytic leukemia. J Clin Invest. 2007; 117:2408–2421. [PubMed: 17717597]
30. Weisman S, Hirsch-Lerner D, Barenholz Y, Talmon Y. Nanostructure of cationic lipid-oligonucleotide complexes. Biophys J. 2004; 87:609–614. [PubMed: 15240493]
31. Nejmeddine F, Raphael M, Martin A, Le Roux G, Moretti JL, Caillat-Vigneron N. ^{67}Ga scintigraphy in B-cell non-Hodgkin's lymphoma: correlation of ^{67}Ga uptake with histology and transferrin receptor expression. J. Nucl. Med. 1999; 40:40–45. [PubMed: 9935054]

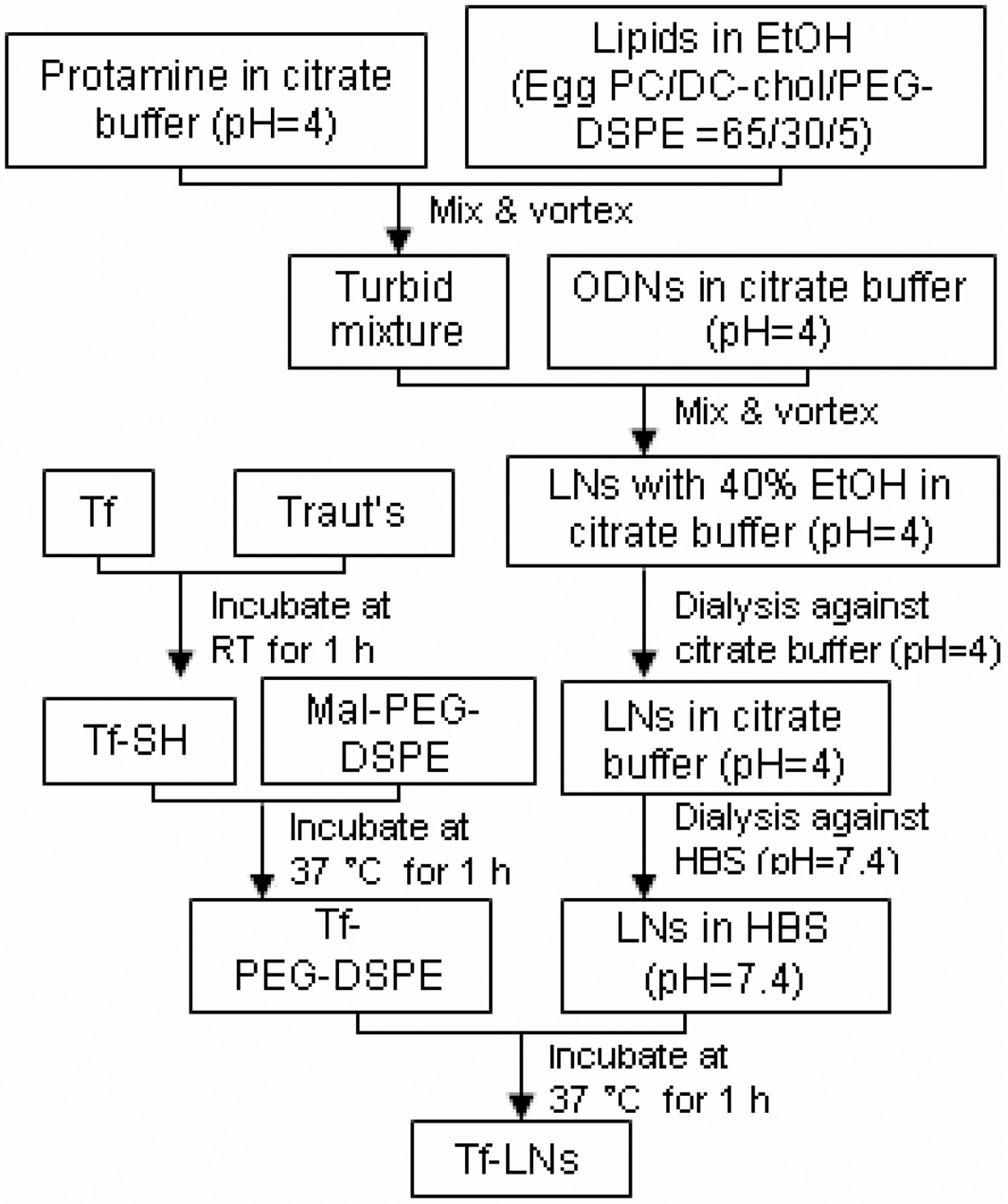

Figure 1.
Schematic illustration of LN synthesis by ethanol dilution and the post insertion of Tf-PEG-DSPE.

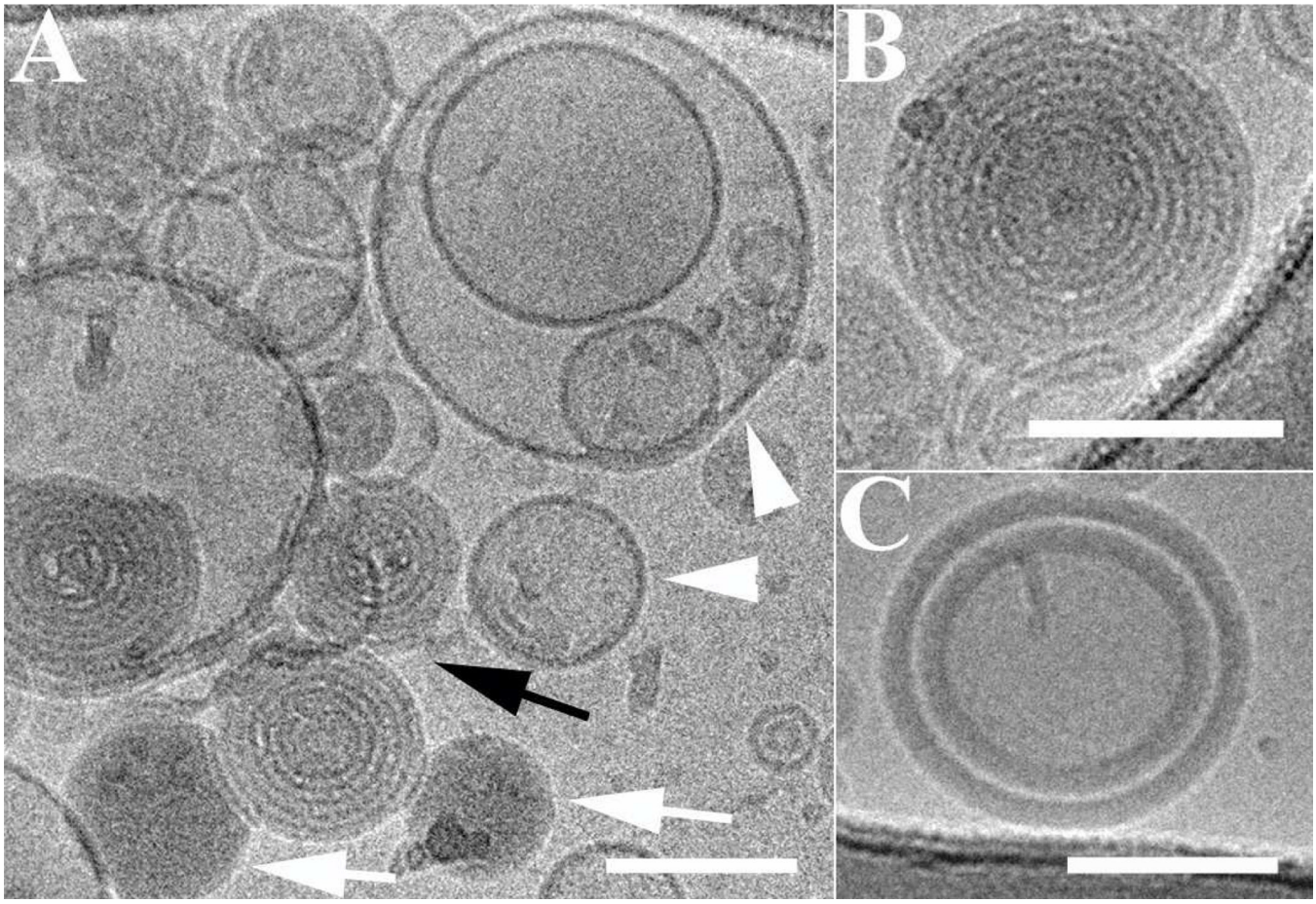

Figure 2.

Cryo-TEM micrographs of LNs entrapping G3139 before transferrin insertion. Scale bars represent 100 nm. (A) Coexisting nanostructures: empty liposomes (white arrowheads), amorphous aggregates of protamine and ODN (white arrows), and onion- like lipoplexes (black arrow). (B) Enlarged, lamellar onion-like aggregate. The ODNs are sandwiched between the lipids bilayers. (C) Concentric multilamellar vesicles with amorphous protamine/ODN layer attached to the surface of the lipid bilayers.

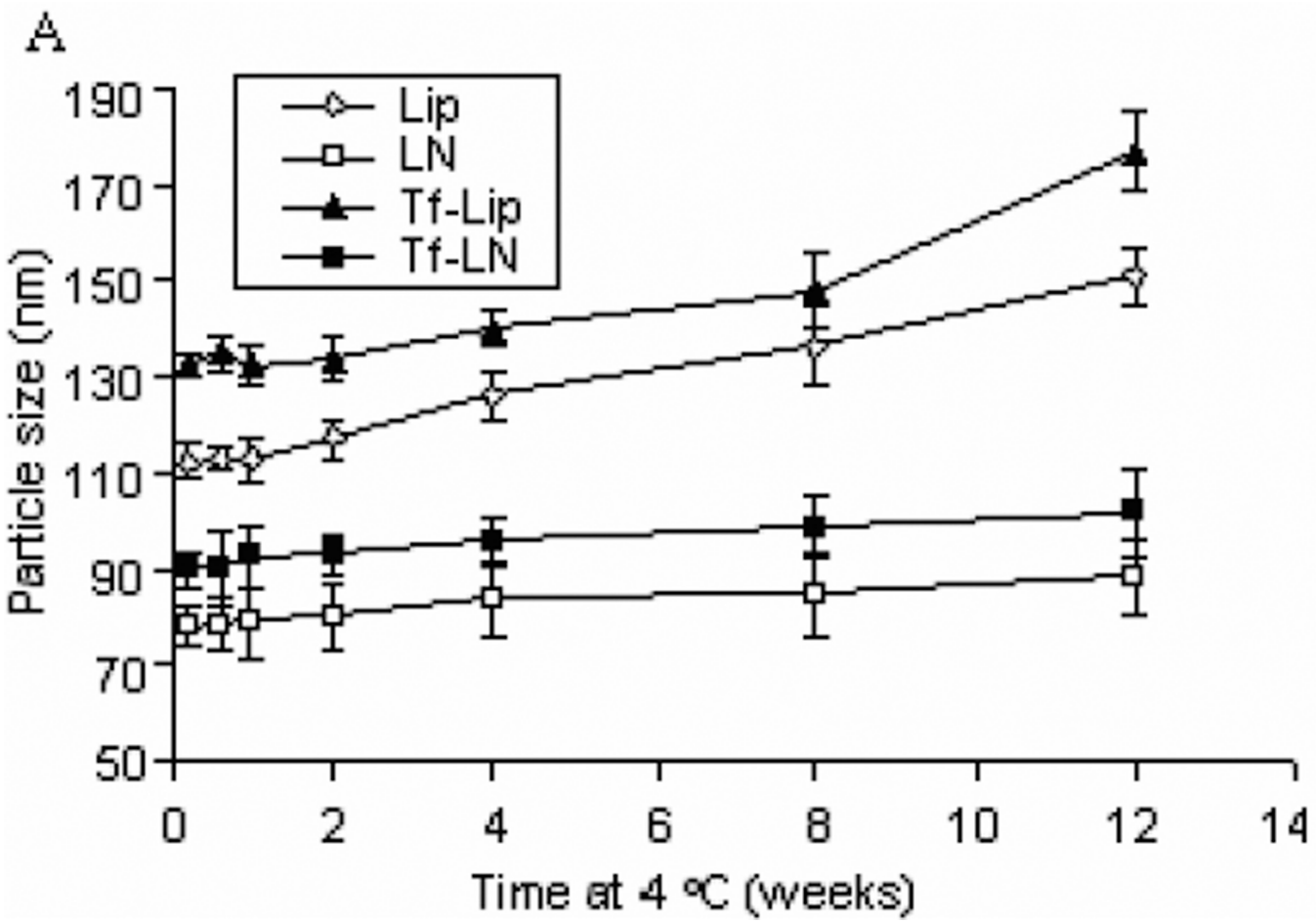

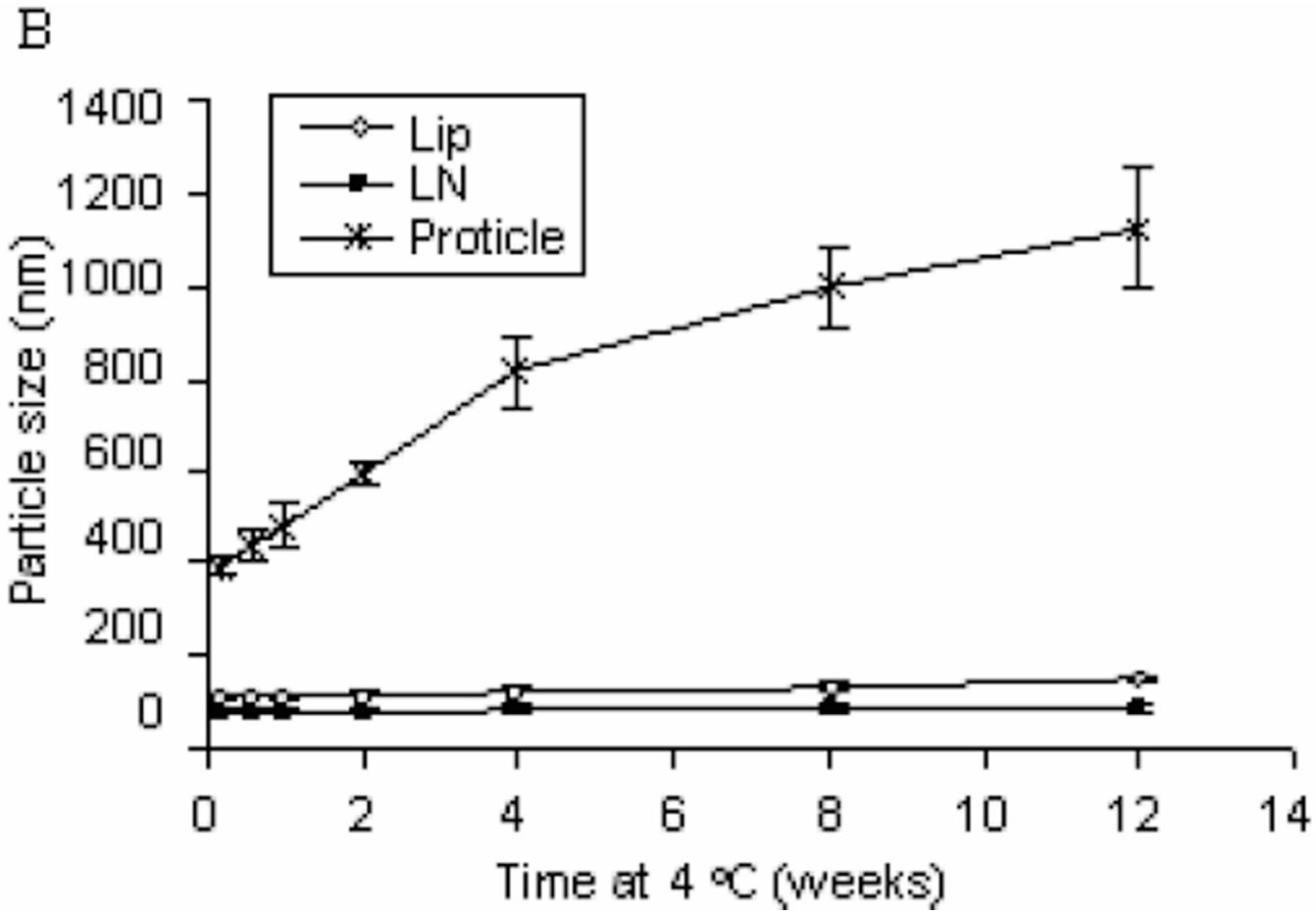

Figure 3.

Colloidal stability of oligonucleotide formulations.

Lip, LN, Tf-Lip,Tf-LN or proticles were stored in HBS buffer at 4 °C and particle sizes were measured by dynamic light scattering. The values in the plot represent the means of 3 separate experiments. Error bars were standard deviations, n=3. Lip, liposomes entrapping G3139; Tf-Lip, Tf-conjugated liposomes entrapping G3139.

Panel A. Colloidal stability profiles of liposomes and LNs.

Panel B. Comparison of colloidal stability profiles of liposomes, LNs, and proticles (protamine-G3139 complexes).

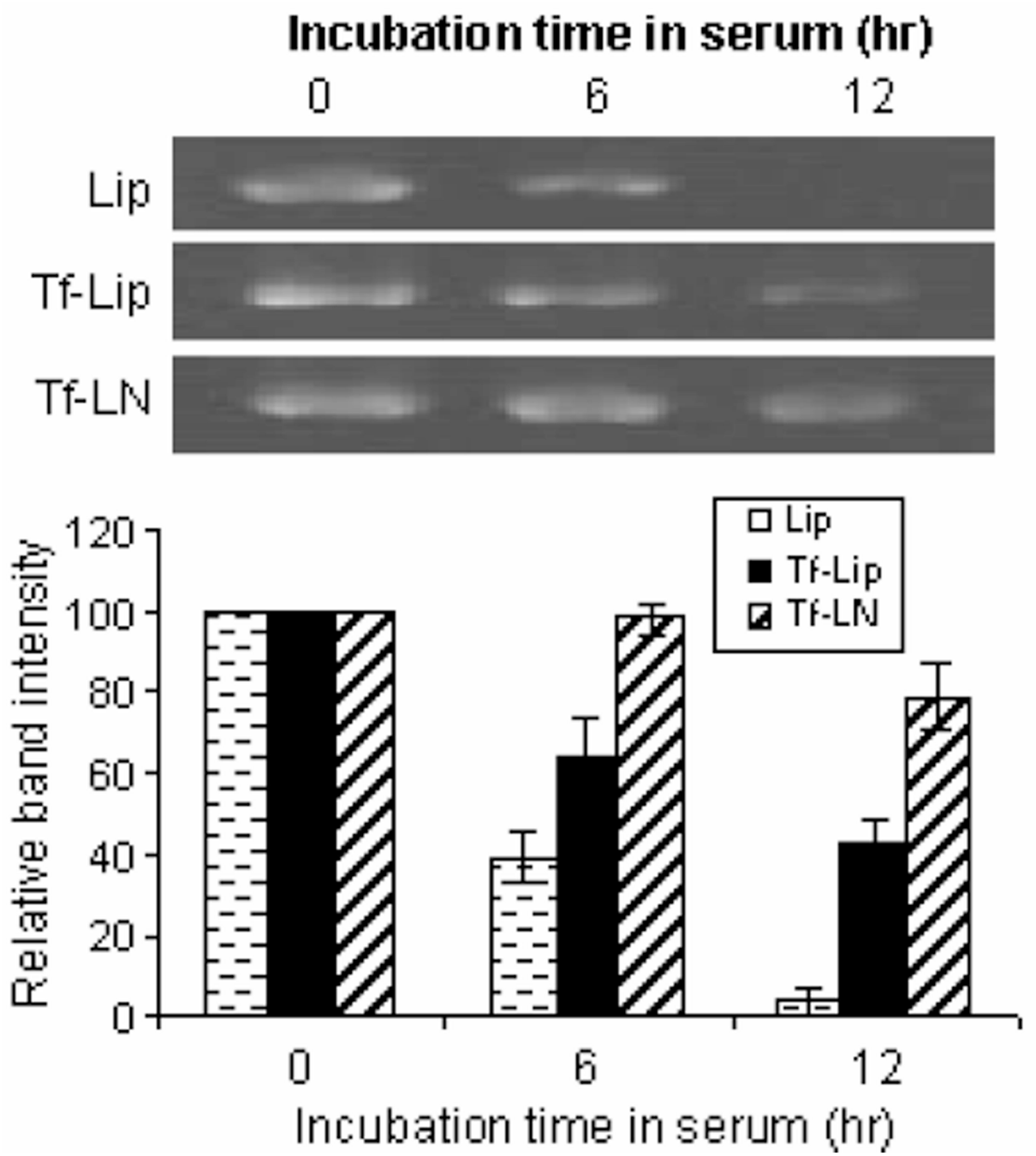

Figure 4.
Serum stability of G3139 in Tf-LNs. Tf-LNs containing G3139 were mixed with serum at 1:4 volume ratio and incubated at 37 °C for different times and were analyzed by urea-PAGE. The density of G3139 bands in urea-PAGE was analyzed by ImageJ. Error bars stand for standard deviations, n= 3.

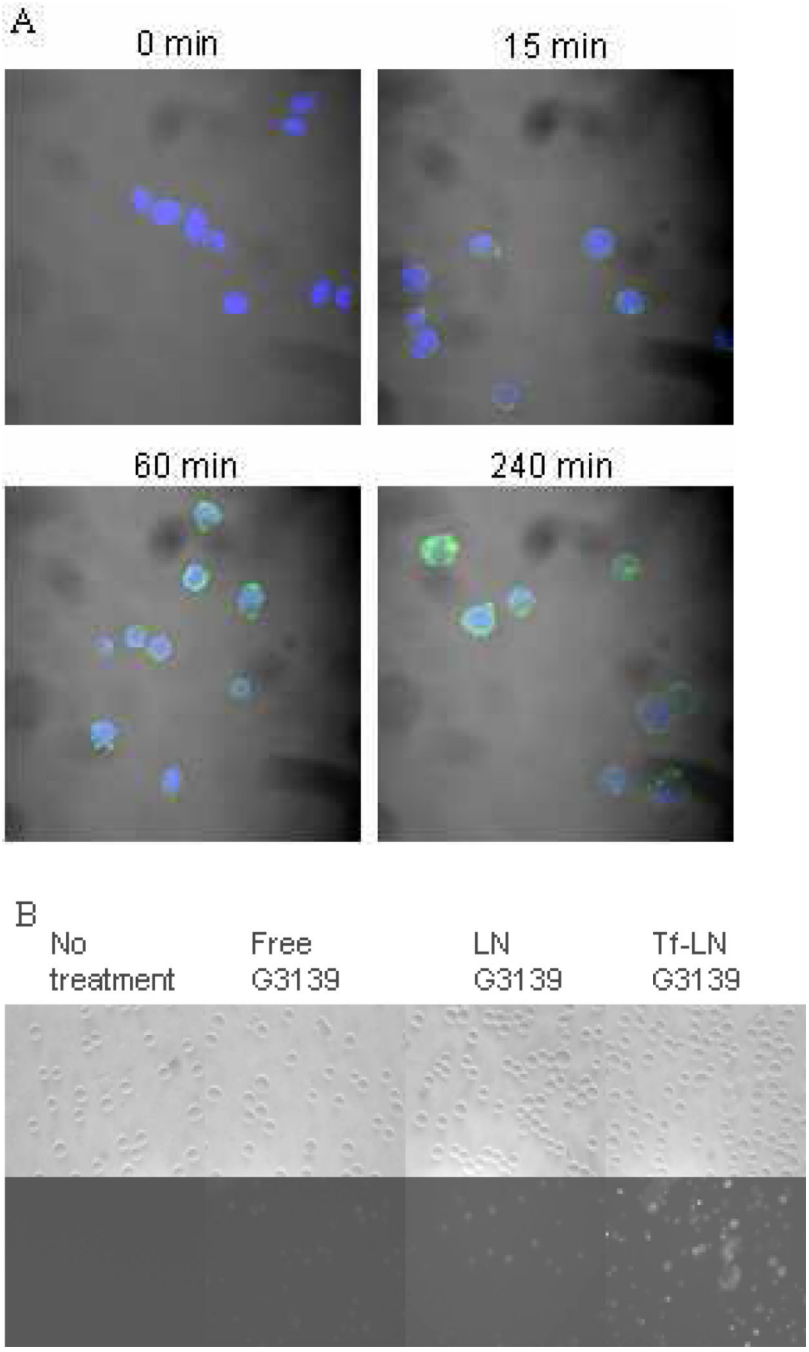

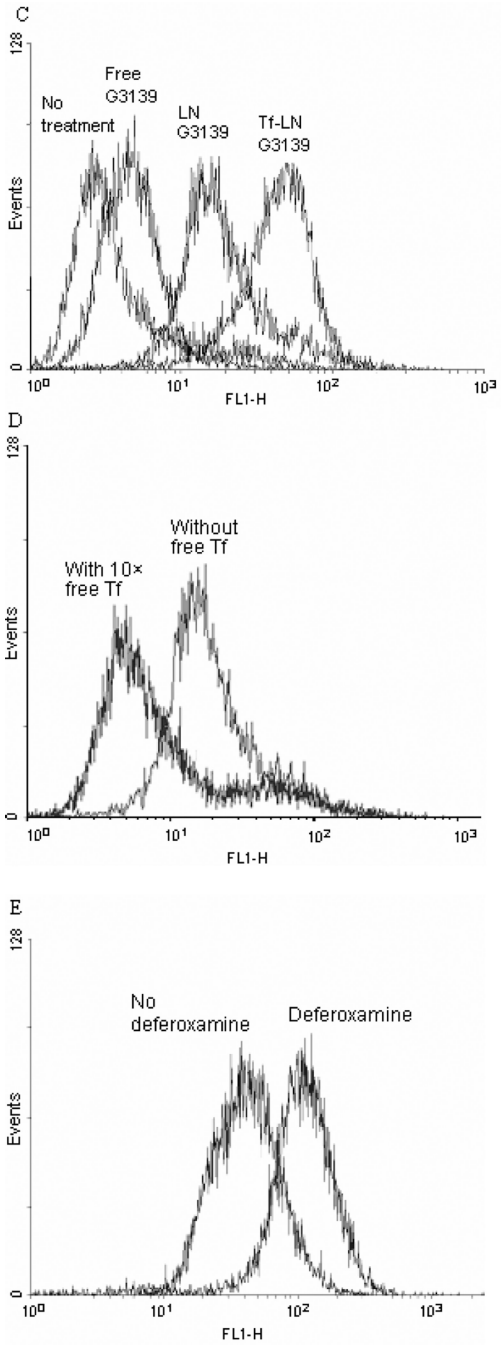

Figure 5.

Uptake of Tf-LN G3139 in MV4-11 cells.

Panel A. Cells were treated with Tf-LN-G3139 spiked with 10% FITC-G3139 (green) at 37°C for 15, 60 and 240 minutes, respectively, stained by DAPI (blue) and visualized on a confocal microscope.

Panel B. Cells were treated with Tf-LN-G3139 spiked with 10% FITC-G3139 for 4 hours at 37°C and visualized on a fluorescence microscope.

Panel C. Cells were treated with Tf-LN-G3139 spiked with 10% FITC-G3139 for 4 hours at 37°C and cellular fluorescence was measured on a FACSCalibur flow cytometery. The X-axis indicates the cellular fluorescence intensity and the Y-axis indicates the cell count.

Panel D. Cells, with or without 10× Tf in the culture medium, were treated with Tf-LNG3139 spiked with 10% FITC-G3139 for 4 hours at 37 °C and cellular fluorescence was measured on a FACSCalibur flow cytometer. The X-axis indicates the cellular fluorescence intensity and the Y-axis indicates the cell count.

Panel E. Cells, with or without pre-incubated with 20 μM deferoxamine, were treated with Tf-LN-G3139 spiked with 10% FITC-G3139 for 4 hours at 37 °C and the fluorescence was measured on a FACSCalibur flow cytometery. Representative results are shown in this histogram with X-axis indicating the cellular fluorescence intensity and the Y-axis indicating the cell count.

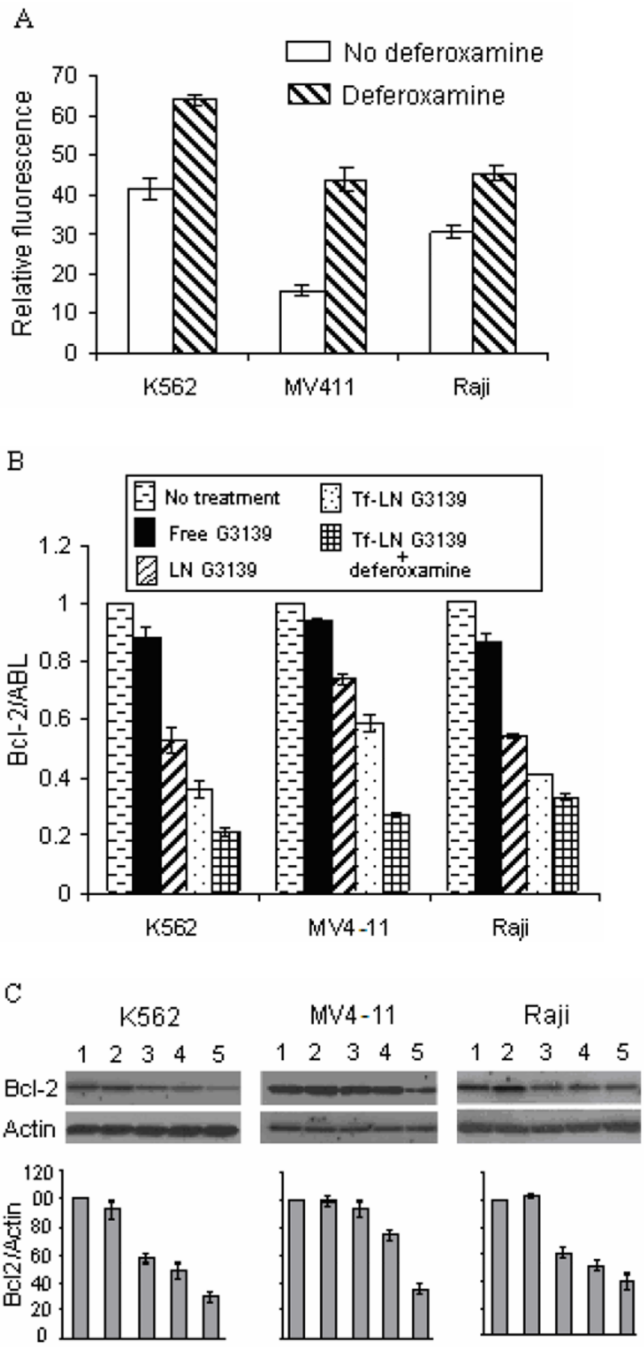

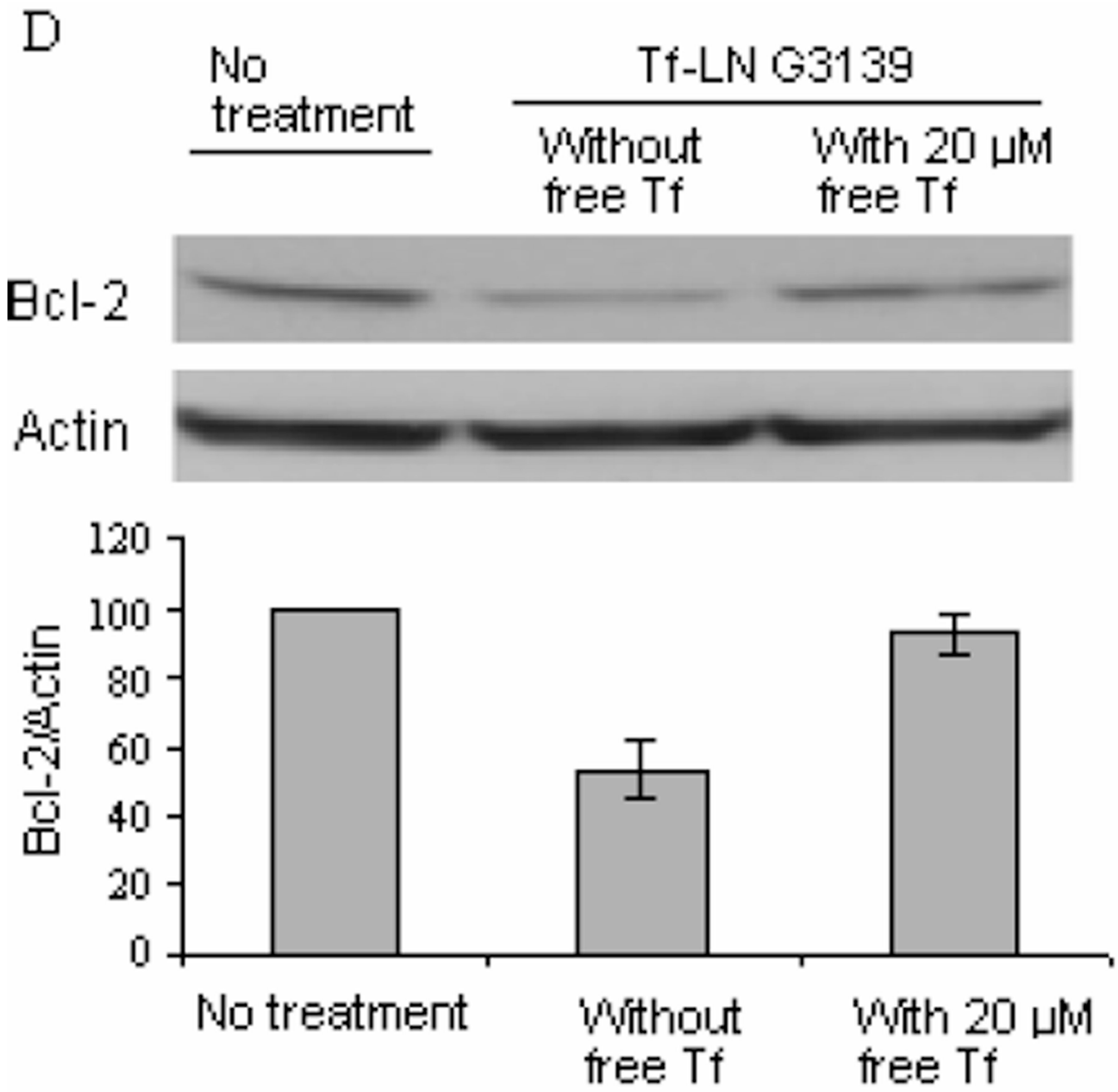

Figure 6.

TfR up-regulation by deferoxamine and its effect on Bcl-2 down-regulation by Tf-LN G3139 in leukemia cell lines.

Panel A. Effect of deferoxamine-treatment on the TfR expression in leukemia cells. Cells were pretreated by 20μM deferoxamine for 18 hours and then with 200 μg/ml FITC-Tf. Cellular fluorescence was measured by flow cytometry. Error bars stand for standard deviations, n= 3.

Panel B. Bcl-2 mRNA down-regulation in different cell lines treated by G3139 in various formulations. Cells were treated with PBS, 1 μM free G3139, G3139 in LN, or G3139 in Tf-LN. In addition, the treatment by Tf-LN G3139 was repeated on cells that were pretreated

with 20 μM deferoxamine for 18 hours. Bcl-2 mRNA levels were quantified by real-time RT-PCR after 48 hours. Error bars stand for standard deviations, n= 3.

Panel C. Bcl-2 protein down-regulation in leukemia cell lines treated by G3139 in various formulations. Cells were treated with PBS (1), 1 μM free G3139 (2), G3139 in LN (3), or G3139 in Tf-LN (4). In addition, treatment by Tf-LN G3139 was repeated on cells that were pre-treated with 20 μM deferoxamine for 18 hours (5). Bcl-2 protein levels were analyzed at 48 hours by Western blot. Upper panel represents the results of Western blot and lower represents its corresponding densitometry data. Error bars stand for standard deviations. Error bars stand for standard deviations, n= 3.

Panel D. Bcl-2 protein down-regulation by Tf-LN G3139 in K562 cells in the presence of 20 μM free holo-Tf in the culture medium. Bcl-2 protein levels were analyzed by Western blot at 48 hours after transfection. Upper panel represents the results of Western blot of Bcl-2 protein expression and lower represents its corresponding densitometry data. Error bars refer to standard deviations, n= 3.

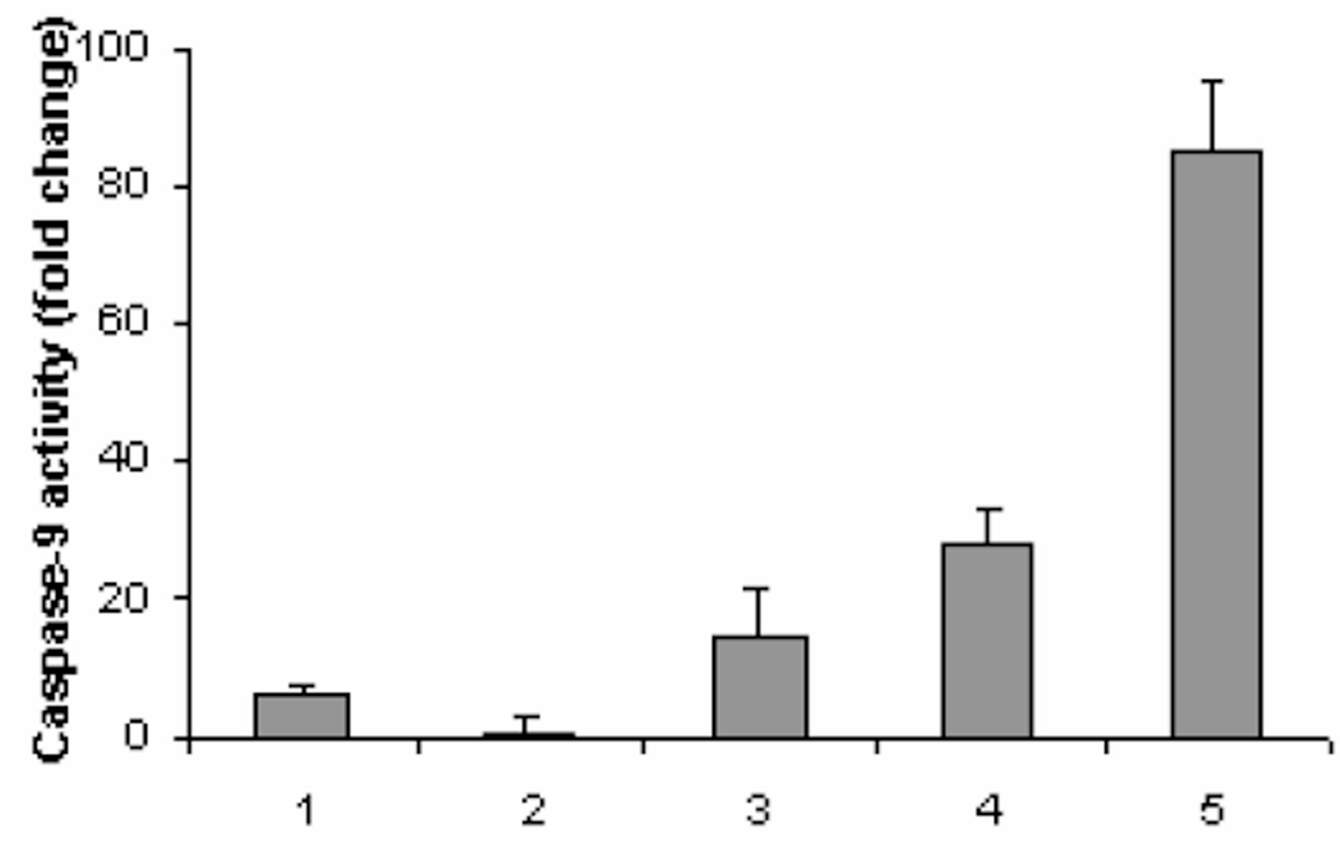

Figure 7.

Apoptosis measured by caspase-9 activities in K562 cells. Cells were incubated with PBS (1), 1 μM free G3139 (2), G3139 in LN (3), or G3139 in Tf-LN (4). In addition, the study was repeated on cells that were pre-treated with 20 μM deferoxamine for 18 hours (5). Cell apoptosis was evaluated via caspase-9 activities, as described in Materials and Methods (n=2).

Table 1

Particle size distribution, zeta potential, and G3139 entrapment efficiency of various formulations [a]

	Particle size (nm)	Zeta potential (mV)	Entrapment efficiency (%)
LN	78.1± 3.4	5.7 ± 0.1	95.9 ± 0.1
Tf-LN	90.2 ± 3.6[b]	5.5 ± 0.6	90.4 ± 0.7[b]
Lip	112.5 ± 4.9[b]	2.0 ± 0.2[b]	76.1 ± 0.2[b]
Tf-Lip	132.5 ± 4.2[b]	1.0 ± 0.4[b]	71.9 ± 1.1[b]

[a] Data represent the mean ± SD (n=3).

[b] $p<0.05$ vs LN group